JOURNAL OF PROPULSION AND POWER
Vol. 16, No. 4, July–August 2000

Comparison of Supersonic Combustion Between Impulse and Vitiation-Heated Facilities

R. R. Boyce*
Imperial College of Science, Technology, and Medicine, London SW7 2BY, United Kingdom
A. Paull,† and R. J. Stalker‡
University of Queensland, Brisbane, Queensland 4072, Australia
and
M. Wendt,§ N. Chinzei,¶ and H. Miyajima**
National Aerospace Laboratory, Kakuda, Miyagi 981-1525, Japan

A comparison has been made between supersonic combustion in two commonly used, but fundamentally different, facilities for scramjet research, a vitiation-heated blowdown tunnel and a free-piston shock tunnel. By passing the shock-tunnel freestream flow through a normal shock and then expanding it to Mach 2.5, combustor inlet conditions and geometries were nominally replicated between the two facilities. A constant-area rectangular duct and a diverging duct, both employing central-strut hydrogen injection, were used. Boundary-layer separation and choking in the constant-area duct limited supersonic combustion comparisons up to a fuel equivalence ratio of the order of 0.3. The experimental results also show that the onset of boundary-layer separation occurs at the same combustor pressure loads and that it behaves similarly in the different facilities. With the diverging duct, comparisons were made up to an equivalence ratio of 1.05. Agreement between the results obtained in the two facilities is within experimental error when the different freestream and boundary layers are accounted for.

Nomenclature

A = cross-sectional area, m^2
C_f = skin friction coefficient
h = specific enthalpy, MJ/kg
M = Mach number
m = mass flux, kg/s
P = pressure, kPa, MPa
Pr = turbulent Prandtl number
q_w = surface heat flux, W/m^2
R = gas constant, m^2/s^2 · K
Re = Reynolds number
T = temperature, K
u = velocity, m/s
x = mole fraction, distance from throat or fuel injection point, mm
γ = ratio of specific heats
δ^* = boundary-layer displacement thickness, mm
ρ = density, kg/m^3
ϕ = fuel equivalence ratio

Subscripts

aw = adiabatic wall value
e = control volume exit plane
i = incipient separation value, control volume inflow plane
w = wedge surface, combustor wall
x = value at distance x
0 = total/stagnation/nozzle reservoir value
∞ = freestream/nozzle exit value
$*$ = throat, reference enthalpy method value

Received 24 January 1998; revision received 25 June 1999; accepted for publication 12 November 1999.

*Research Fellow, Centre for Dynamics; currently Research Fellow, Department of Aeronautics, University of Queensland, Brisbane, Queensland 4072, Australia. Member AIAA.
†Senior Research Fellow, Centre for Hypersonics, Mechanical Engineering. Member AIAA.
‡Emeritus Professor, Centre for Hypersonics, Mechanical Engineering. Member AIAA.
§STA Fellow, Kakuda Research Center; currently Research Engineer, Commonwealth Scientific and Industrial Research Organisation, Division of Exploration and Mining, Kenmore, Queensland 4069, Australia.
¶Head, Kakuda Research Center, Research Coordination Office.
**Director, Kakuda Research Center.

Introduction

SUPERSONIC combustion experiments for scramjet development are generally performed in ground-based facilities. These are typically either vitiation-, arc-, or storage-heated tunnels, which have flow times of the order of seconds or longer, or impulse facilities such as free-piston shock tunnels, with flow times of the order of milliseconds. The long-duration facilities are capable of testing up to a flight Mach number of 8, whereas the impulse facilities are most useful beyond Mach 8. Supersonic-combustion experiments in each type of facility meet with problems/phenomena that are peculiar to each and that differ from real flight. Among the long-duration facilities described, the vitiation-heated ones are relatively simple and easy to operate compared with the other facilities such as the arc-heated ones (where very high-power electric supplies are necessary and considerable NO contamination due to the arc is unavoidable) or the storage-heated ones, where a very large storage heater is necessary and a long preparation period for heating prior to runs is required. This has resulted in extensive combustor data being generated in vitiation-heated tunnels. However, the vitiation-heated blowdown tunnel delivers air to the combustion chamber with the presence of large concentrations of H_2O. On the other hand, shock tunnels produce freestreams with quantities of NO and O at flight Mach numbers greater than 10. Furthermore, because of the short flow duration, there has been some doubt whether or not effects such as thermal choking and boundary-layer separation can be properly reproduced in impulse facilities. The importance of these effects needs to be understood to use each type of facility confidently for scramjet research. In particular, if ground-based experiments are to be made beyond Mach 8, impulse facilities are at present the only viable option. Thus, it is important to verify, at low flight speeds, that results from impulse facilities agree with those from longer-duration facilities.

As pointed out by Mitani et al.,[1] much numerical work has been performed to assess the effect of vitiated air on combustion. For example, Mitani[2] showed that the presence of H_2O produces an ignition delay for reaction pressures of the order of 100 kPa or

more, for H_2O mole fractions of the order of 0.2 or more. Until very recently, however, experimental comparisons of supersonic combustion between different types of facility had not been reported in the literature. Guy et al.,[3] comparing arc-heated and vitiation-heated scramjet experiments at Mach 4–5, reported reduced thrust for the vitiation experiments. Similarly, Mitani et al.[1] reported reduced thrust in Mach 6 vitiation-heated experiments, as compared with storage-heated experiments. With the effects of vitiation on thrust production established, a meaningful comparison of the performance of a supersonic combustor in vitiation-heated and impulse facilities can be made. As the comparison can only be made at the lower end of the shock-tunnel operating regime, the shock-tunnel freestream will not be contaminated by NO or O. Noting any differences produced by vitiation, the comparison, thus, will establish the effect of flow duration on thrust production and the development of structures such as separation bubbles.

To this end, a collaborative project between Australia and Japan has been undertaken to compare supersonic combustion of hydrogen in both types of facility. In Japan, measurements were made using a Mach 2.5 vitiated-air generator blowdown tunnel (VAG)[4] of the Kakuda Research Center, National Aerospace Laboratory (NAL). In Australia, the free-piston shock tunnel T4 (Ref. 5) of the University of Queensland (UQ) has been used. This paper compares static pressure results from similar combustor configurations installed in both facilities.

Experiment

Ideally, experiments in the two facilities would exactly replicate all factors such as the flow conditions and geometry. However, the fundamental difference in gas composition means that not all flow conditions can be matched. A choice must be made as to which conditions should be matched, so that the fluid dynamics and combustion processes flow are as close as possible between the two facilities. For the fluid dynamics, the Mach number M is chosen and is controlled primarily by geometry. For combustion, various parameters are important: The static pressure P and temperature T influence reaction rates, the total temperature T_0, which has a large effect on the static temperature, may influence ignition processes in stagnation regions or near walls, and the mass flux determines how much fuel is burnt for given fuel–air equivalence ratios. For the present work, P and T_0 were chosen partly for their importance and partly because they are more readily determined experimentally than other parameters. Nominal conditions of $M = 2.5$, $P = 60$ kPa, and $T_0 = 2200$ K were chosen. There are differences in the other parameters (and in the actual, rather than target, values achieved for M, P, and T_0), and the results from each facility are correlated using analytical and computational methods.

The combustor and fuel-injector configurations were kept as simple as possible. Two different combustion-chamber configurations have been tested: a constant-area rectangular duct with nominal cross-sectional dimensions 50 × 100 mm and variable length and a diverging rectangular cross section duct. Central-strut hydrogen injection was used.

The experiments in the vitiation-heated tunnel were performed in a standard manner for that tunnel, with the combustor directly connected to the tunnel nozzle and the flow conditions produced by the tunnel being the combustor inlet conditions. On the other hand, the experiments in the shock tunnel involved an extra degree of complexity because the flow conditions produced by the shock tunnel were too high in total pressure and Mach number. To achieved the desired Mach number and total pressure, the flow from the shock-tunnel nozzle was processed through an inlet that was choked (to reduce the total pressure) and then through a supersonic nozzle (to produce the desired Mach number). The nozzle was directly connected to the combustor[6] as in the VAG, but the nozzle used in T4 was much shorter.

Vitiation-Heated Experiment at NAL

VAG, used in the present work at NAL,[4] is shown in Fig. 1a. Air and additional quantities of O_2 and H_2 are mixed in a subsonic combustion chamber to generate a combustion gas containing the same mole fraction of O_2 as pure air. After ignition (by a spark plug) and burning, the mixture becomes the reservoir for a 180-mm-long (throat to exit), two-dimensional contoured nozzle of nominal exit Mach number 2.5. The maximum total temperature, enthalpy, and pressure attained by the reservoir gas is 2700 K, 4.2 MJ/kg, and 1.5 MPa, respectively. The nozzle has throat dimensions of 32 × 51 mm and exit dimensions of 94.3 × 51 mm. Scramjet combustors are directly connected to the exit of the tunnel nozzle, to examine the combustor independently of the scramjet inlet. The scramjet flow exhausts directly into the atmosphere. Flow duration is approximately 7 s, with steady flow occurring for 4 s. This flow duration results in significant heating of components exposed to the flow. Water cooling is thus used for sharp and small-radius leading edges.

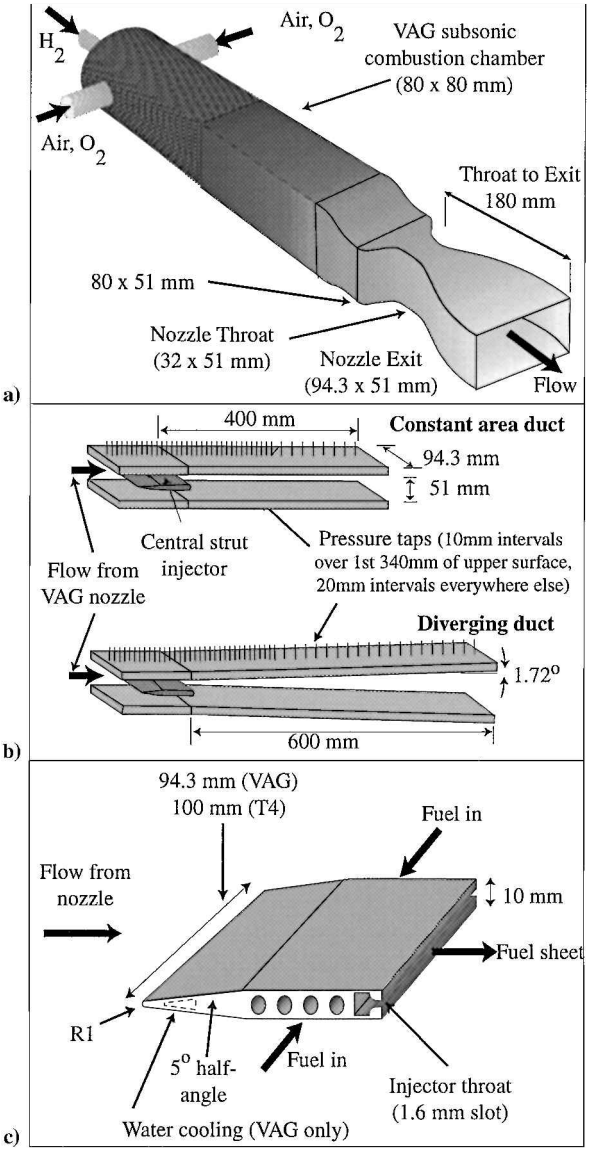

Fig. 1 a) VAG schematic, b) VAG scramjet combustors, and c) fuel-injector, VAG and T4.

The nozzle reservoir (subscript 0) and exit (subscript ∞) conditions in the VAG for the present work are given in Table 1. The T4 flow conditions are also presented in Table 1, for comparison, and are described later. The exit conditions were calculated using the inviscid one-dimensional equilibrium-chemistry ODE program.[7] The nozzle exit conditions are the scramjet inlet conditions in the VAG experiments and correspond to a flight Mach number of approximately 8. Of particular importance is the very large water mole fraction, which is typical of vitiation-heated facilities, but very different to the real flight situation.

The two combustor configurations employed in the present work are shown for the VAG in Fig. 1b, a constant area rectangular duct with length 400 mm and a diverging (1.72-deg divergence

half-angle) rectangular cross section duct with length 600 mm. The leading edge of the fuel injector is located 43 mm downstream of the nozzle exit. The plane of the injector is the same as the plane in which the VAG nozzle expansion occurs. Centerline pressure taps (shown in Fig. 1b) are connected to a pair of 48-channel Scanivalve Corporation rotary pressure scanners via plastic tubing. The pressure at each location was sampled and averaged in turn, for 40 ms each, over a 2-s period during the VAG steady flow duration, yielding one data point per pressure tap per run.

The fuel-injector geometry employed in the VAG is shown schematically in Fig. 1c. It consisted of a 10-mm-thick strut with a 5-deg half-angle blunted wedge on the upstream side to deflect the oncoming flow. Earlier experiments at NAL with a 10-deg half-angle wedge resulted in separation of the thick boundary layer on the wall of the duct adjacent to the injector,[4] with subsequent choking of the duct. Computational work[4] indicated that the boundary-layer separation due to the strength of the shock impinging on the wall would occur for half-angles greater than 7 deg. The leading-edge radius was 1 mm. The dashed line in Fig. 1c shows the location of the water cooling channel for the VAG injector. Fuel enters the injector from both sides, is delivered evenly through directional channels to the rear of the injector, and exits as a continuous sheet that spans the scramjet combustor. A two-dimensional throat at the injector exit was used to get sonic injection. The fuel mass flux (and also the VAG air, O_2, and H_2 flow rates) were calculated by monitoring the flow through standard sharp-edged orifices with differential pressure gauges during each run.

Table 1 VAG and T4 flow conditions

Parameter	VAG	T4
T_0, K	2214 ± 2%	2105 ± 6%
h_0, MJ/kg	2.79 ± 1%	2.40 ± 6%
P_0, kPa	1012 ± 1% (meas.)	1035 ± 5% (meas.)
M_∞	2.44 ± 0.2%	2.47 ± 6%
P_∞, kPa	59 ± 1% (meas.)	59 ± 9% (meas.)
T_∞, K	1258 ± 2%	1025 ± 13%
u_∞, m/s	1753 ± 1%	1560 ± 4%
m_{O2}, kg/s	0.33 ± 0.01	0.35 ± 0.02
γ_∞	1.28 ± 0.2%	1.39 ± 0.01
R_∞	321 ± 0.3%	287.1
x_{N2}	0.485 ± 0.006	0.79
x_{O2}	0.210 ± 0.005	0.21
x_{H2O}	0.299 ± 0.006	0.0
x_N, x_O, x_{NO}	0.0	0.0

Free-Piston Shock-Tunnel Experiment at UQ

The free-piston shock tunnel[5] operates by using a free piston to compress the driver gas between the piston and a diaphragm separating the compression tube and the shock tube (containing the test gas). The compressed driver gas ruptures the diaphragm, producing a shock wave that propagates along and reflects from the shock tube end wall, leaving a stagnant high-enthalpy reservoir of test gas. This reservoir feeds through an axisymmetric contoured nozzle into a test section and dump tank, which are evacuated prior to the tests. By suitable choices of the driver operating conditions, primary diaphragm thickness, and shock-tube initial pressure, T4 is capable of nozzle reservoir enthalpies and pressures in the ranges 2–15 MJ/kg and 10–80 MPa, respectively. For the present work, the lowest end of both the enthalpy and pressure capabilities was required. At these conditions, the test time is approximately 5 ms. A contoured nozzle that delivers parallel flow at nominally Mach 4.5 was used. The test core of this nozzle at the location of the scramjet intake is approximately 100 mm in diameter. A contoured nozzle that produced a Mach 2.5 flow could not be used in these experiments because the test core diameter would have been significantly smaller than the intake of the combustor.

Scramjet combustor tests are normally performed in the shock tunnel in cookie cutter mode, where the tunnel freestream flows directly into the combustor and the boundary layer of the nozzle is spilled outside the combustor. Thus, the combustor inlet total pressure is the reservoir pressure of the hypersonic nozzle, which is greater than 10 MPa. To match both the VAG combustor inlet conditions ($M_\infty = 2.44$, $P_0 = 1.012$ MPa, and $T_0 = 2214$ K) and dimensions, a different arrangement was necessary. An unstarted 96-mm-long two-dimensional converging–diverging Mach 2.5 nozzle was employed, mounted 80 mm downstream of the Mach 4 nozzle exit at tunnel recoil and directly connected to the combustor (Fig. 2). Unlike the VAG, the plane in which the expansion to Mach 2.5 occurs is orthogonal to the injector plane of symmetry. The successful operation of this inlet (detailed elsewhere[6]) is summarized next.

Briefly, a pair of wedges were employed that initially produced an oblique shock system in the inlet. The reflected-shock impingement on the wedges forced boundary-layer separation that, in turn, caused inlet unstart. As a result, the subsonic flow in the inlet provided the reservoir for the Mach 2.5 nozzle, which was located downstream of the choked inlet. Shock-tunnel operating conditions were chosen such that the freestream pitot pressure equaled the desired combustor inlet total pressure (≈ 1 MPa). Surface pressure measurements in the inlet, P_w, throat, P_*, and exit, P_∞, of the Mach 2.5 nozzle, as well

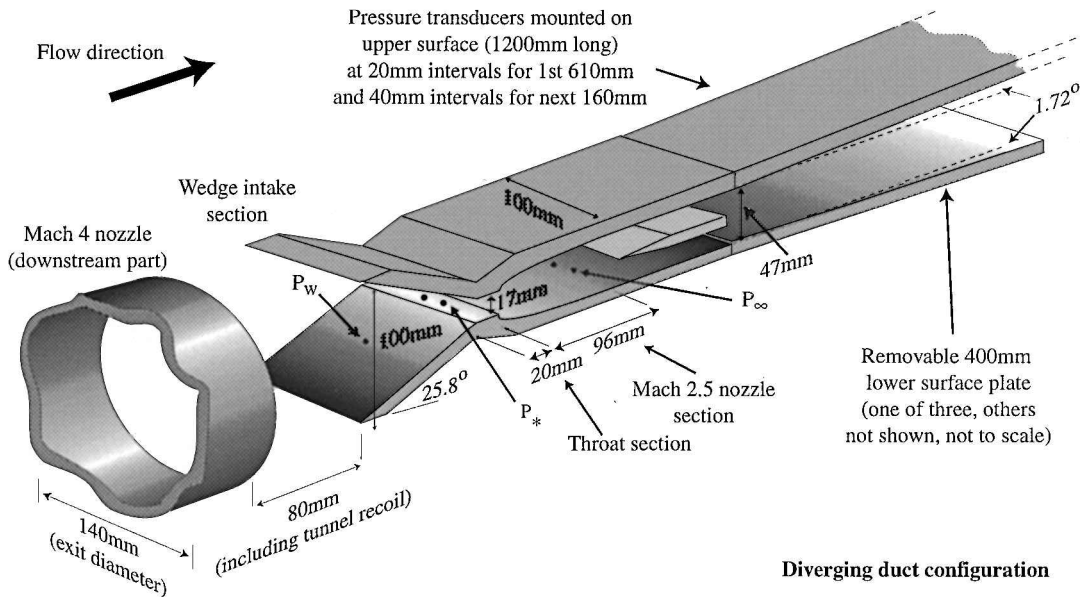

Fig. 2 T4 scramjet configuration.

as pitot pressure P_{pitot} measurements at the nozzle exit, were used to confirm the behavior of the inlet and to determine the flow conditions at the entrance to the combustor.

The T4 combustor inlet conditions are summarized in Table 1 and were determined by first using the equilibrium-chemistry shock-tube code ESTC,[8] along with the measured tunnel nozzle reservoir pressure and primary shock speed, to calculate the total temperature and enthalpy. The freestream properties produced by the nozzle connected to the shock tube were determined from the measured reservoir pressure and the calculated total temperature using the non-equilibrium one-dimensional code NENZF.[9] Calculations of the Mach 2.5 nozzle flow were made by again using NENZF and matching the predicted pitot pressure with that measured at the Mach 2.5 nozzle exit. A more in-depth study of the flow conditions is detailed elsewhere.[6]

Noted that whereas chemical effects are unimportant at these low-enthalpy conditions, vibrational relaxation is important, and yet the extent of the relaxation is unknown. Hence, the flow conditions at the exit of the Mach 2.5 nozzle are taken to be the mean of the calculated values for the two extremes of vibration. It was observed that if the measured value of P_∞ / P_0 was used to evaluate the vibrational state then the scramjet inlet conditions were more aligned with the frozen vibration predictions than shown in Table 1. In particular, the static temperature was lower, approximately 930 K, and the Mach number was higher, approximately 2.53. The flow conditions correspond to a flight Mach number of approximately 6.9.

The T4 total enthalpy and temperature are somewhat lower than the VAG conditions (14 and 5%, respectively), a result of the chosen shock-tunnel conditions. At the higher primary shock speeds that would provide closer matching of the VAG conditions, the behavior of the unstarted inlet was unstable, and so a slightly lower shock speed was selected.

The scramjet configurations used in the shock-tunnel experiments were the same as in the VAG, except that the constant area duct (and upstream end of the diverging duct) cross section had the dimensions 47×100 mm. The upper surface was 1200 mm long, instrumented with piezoelectric pressure transducers along the centerline (see Fig. 2). The lower surface had a variable length in multiples of 400 mm. To alter the constant-area duct length (to investigate the influence of the boundary layer), one or more sections of the lower surface were removed, relieving the pressure on the boundary layer in the duct downstream of that point. This effectively eliminated the possibility of choking due to boundary-layer separation in that region.

The fuel injector used in T4 was nominally identical in geometry to the one in the VAG, except that it did not contain any water cooling channels. The flow of fuel through the injector was initiated by opening a fast-acting valve.[10] A signal from a displacement transducer monitoring the recoil of the shock tunnel is used to trigger the valve, which remains open for approximately 20 ms. Thus, the scramjet combustor is filled with hydrogen prior to the arrival of air in the test section, and this fuel must be pushed out by the air before steady flow can occur. A pressure transducer was used to monitor the fuel pressure upstream of the injector. This pressure is proportional to the mass flux of hydrogen through the injector. The proportionality constant (dependent on the injector throat size and determined experimentally[11]) was used to determine the mass flow rate of the fuel during the experiments.

Theoretical Analysis

Because there are some differences between the combustion chamber entrance freestream conditions, it is expected that there will be differences between the experimental results. To develop the expected correlation between these measurements, a quasi-one-dimensional equilibrium chemistry control volume analysis has been performed in which the effects of boundary-layer displacement, wall-surface heat transfer, and skin friction are accounted for.

The inflow boundary of the control volume is fixed at the injector exit plane, whereas the outflow boundary location is marched downstream from the injector to determine the expected pressure at these locations. The combustor walls form the other control volume boundaries.

The calculations proceed by first specifying the velocity, static temperature, static pressure, and composition of the freestream (recalling that the VAG has a high H_2O concentration) that enters the combustor upstream of the injector. The fuel–air equivalence ratio, fuel–air area ratio, and fuel total temperature are also specified along with the distance x over which the boundary layer on the duct walls has grown [starting from the nozzle throat and ignoring the injector (under the assumption that the compression/expansion effect of the injector causes zero contribution to boundary-layer growth)]. It is then assumed that the fuel is injected sonically. This gives the fuel stream pressure, velocity, and temperature at the exit of the injector. The freestream properties of a uniform mixture of the air and fuel (without combustion) are then obtained by assuming that mixing occurs instantaneously and at constant volume. These freestream properties are used as the conditions at the inflow boundary of the control volume. The final inflow parameter required is the effective area of the inflow boundary, which is determined by reducing the wall dimensions there by the turbulent boundary-layer displacement thickness δ^*. This is different in both facilities (because the Mach 2.5 nozzles are of different lengths) and is important to estimate the pressure rise in both facilities.

Shapiro[12] supplies tabulated data for δ^*/δ for turbulent boundary layers, for which an accurate curve fit over the Mach number range 1.0–3.2, combined with Edenfield's Mach 8 nozzle turbulent boundary-layer thickness correlation,[13] yields

$$\frac{\delta^*}{x} = \frac{0.2145 M^{0.375}}{Re_x^{0.166}}(0.08801M + 0.06385) \tag{1}$$

The Reynolds number for the VAG is calculated using the coefficient of viscosity for standard, rather than wet, air. Computations for the viscosity of air with water content of up to 5% at 1200 K show less than 1% variation in the coefficient of viscosity.[14] That result, combined with the weak dependence of δ on Reynolds number, makes this a reasonable assumption. Note that just upstream of the injector, Eq. (1) gives $\delta^* = 1.8$ mm for the VAG and $\delta^* = 0.9$ mm for T4, with the difference being mainly due to the VAG's greater nozzle length.

To determine the equilibrium combustion properties along the duct, that is, different outflow boundary locations, the one-dimensional equations of motion are solved simultaneously.

Continuity:

$$\rho_i u_i A_i = \rho_e u_e A_e \tag{2}$$

Momentum:

$$P_i A_i + \rho_i u_i^2 A_i + \int_i^e P \, \mathrm{d}A - \frac{1}{2}\int_i^e \rho u^2 C_f \, \mathrm{d}A_w = P_e A_e + \rho_e u_e^2 A_e \tag{3}$$

Energy:

$$\rho_i u_i A_i \left(h_i + \frac{u_i^2}{2}\right) - \int_i^e q_w \, \mathrm{d}A_w = \rho_e u_e A_e \left(h_e + \frac{u_e^2}{2}\right) \tag{4}$$

In the momentum equation, the third and fourth terms are the total axial pressure and viscous forces acting on the control volume boundaries other than the inflow (subscript i) and outflow (subscript e) boundaries. In the energy equation, the second term represents the total heat added through the side walls. A_w is the wall surface area. The skin friction coefficient C_f and wall surface heat flux q_w are determined using the reference-enthalpy method described by Heiser and Pratt[15]:

$$C_f = \frac{0.0574}{Re_x^{*2}} \frac{T}{T^*} \tag{5}$$

$$q_w = \frac{0.0287 Pu(h_{\text{aw}} - h_w)}{RT^* Pr^{*0.4} Re_x^{*0.2}} \tag{6}$$

where superscript asterisk denotes quantities determined at the reference enthalpy.[15] The wall temperature used here is 300 K for T4

(essentially room temperature) and 1000 K for the VAG (because of the long flow duration, this was chosen arbitrarily to be approximately the mean of room temperature and the melting temperature of the copper walls of the VAG combustor; as will be seen later, the choice is not important to first order). The given system of equations is closed with the usual equation of state and with empirical data[16] for the species specific heats, enthalpies of formation, and equilibrium constants.

Initially, the inflow and outflow boundaries lie in the same plane, and so dA_w is zero and there are no losses from the control volume due to viscous drag or surface heat flux. For this control volume, the equations are solved by assuming a value for A_e. Writing the axial pressure force for this case as $0.5(P_i + P_e)(A_e - A_i)$, the system of governing equations is then solved iteratively to yield values for u_e, ρ_e, P_e, h_e, T_e, and the species composition. A new displacement thickness is then calculated, providing a new value for A_e, and so on until the computed displacement thickness converges (usually requiring only a few iterations). By the using of this method, the equilibrium combustion conditions at the start of the combustor are thus determined, accounting for compression of the boundary layer by the increased pressure.

The control volume outflow boundary is then marched down the duct, so that the losses due to skin friction and surface heat transfer gradually accumulate as A_w increases. At each duct location, C_f and q_w are calculated using the conditions determined from the previous location, with the distribution of conditions along the duct to that point being used to evaluate the axial pressure forces and the surface heat flux for the current control volume. With these additions, the governing equations are solved as earlier. For verification purposes, the algorithm described has been used to compute a perfect gas supersonic expansion with coarse steps, with the result that it reproduced the exact area ratio–Mach number variation to within 0.4% everywhere.

Because the true three dimensionality of the flow (including shocks) is not accounted for and because the impact of finite rate mixing and chemical kinetics is also ignored, this analysis is expected to be most useful in the far field, where the injector shock system has become sufficiently smeared by its interaction with the boundary layer and where mixing and kinetics have both attained equilibrium. As a result, it provides a means to access the extent of the mixing and kinetics in each facility by the deviation of the theoretical analysis from experimental data. It also enables the effects of the different combustor inlet conditions in each facility to be accounted for in the experimental data and enables the relative importance of skin friction, surface heat flux, boundary-layer displacement, and also vitiation to be assessed.

The analysis also gives the frozen Mach number and so can indicate the approximate ϕ above which thermal choking would occur for equilibrium combustion. For the parameters of Table 1, thermal choking is expected for $\phi > 0.80$ in the VAG and $\phi > 0.61$ for T4.

Results

Throughout the experiments, the flow conditions given in Table 1 were maintained, and the fuel equivalence ratio ϕ was varied by varying the hydrogen mass flux through the injector.

Data Analysis

For the VAG, data analysis was automated, with the mean pressure at each pressure tap during steady flow, plus the fuel mass flow rate, determined by preprogrammed software.

Data analysis for the T4 results proceeded as follows. The pressure time histories along the duct, in the Mach 2.5 nozzle and in the fuel system, were recorded and individually processed. Figure 3 shows two sample pressure histories in the constant area duct for a run with fuel equivalence ratio $\phi = 0.47$. The first trace is for a position 110 mm downstream of the injector exit and displays jagged features that represent transient (or at least nonstationary) shocks moving across the transducer. The second trace, recorded 390 mm downstream of the injector exit, exhibits a very stable pressure history after the tunnel and duct startup period (~1.5 ms). The startup period corresponds to the unstarted inlet startup period.[6] This stability is typical of measurements well downstream of the injector, for both ducts. The pressure at a given location was determined by choosing the time at which P_0 was equal to 1035 kPa, typically approximately 2.5 ms after the start of flow in the scramjet. The mean pressure in a 2-ms window around that time was then determined. The 2-ms window was chosen to attempt to average out the effects of transient features. A comparison for the pressure distribution along the constant-area duct for the same run as in Fig. 3, between a 2-ms and a 0.05-ms averaging window, is shown in Fig. 4. This comparison shows that near the front of the duct, where pressure history fluctuations due to shocks are important, the larger window has a strong effect on smoothing the pressure distribution. There is little difference between the two windows over the downstream part of the duct. Use of the 2-ms window more closely matches the long (40-ms) VAG averaging period, where transient features can not be observed.

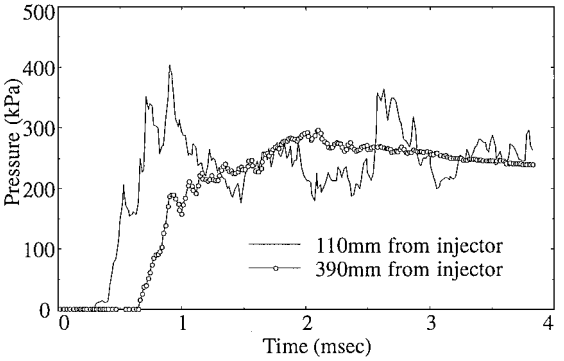

Fig. 3 T4 transient features.

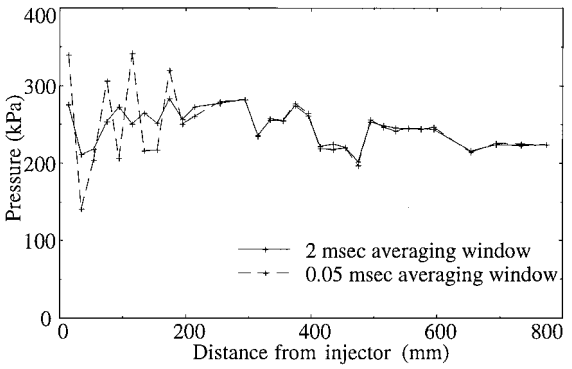

Fig. 4 T4 averaging window comparison.

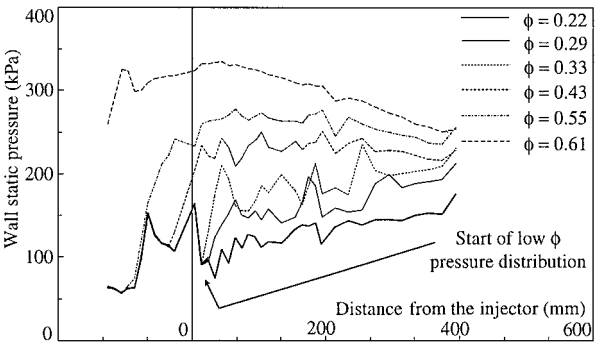

Fig. 5 VAG constant-area duct pressure distributions.

Constant-Area Duct Results

The measured pressure distributions along the constant-area duct in the VAG experiment are presented in Fig. 5, for various fuel equivalence ratios. For the low-fuel-equivalence-ratio cases, the pressure upstream of the injector (59 kPa) and the shock system around the injector can be seen. Farther downstream, a gradually

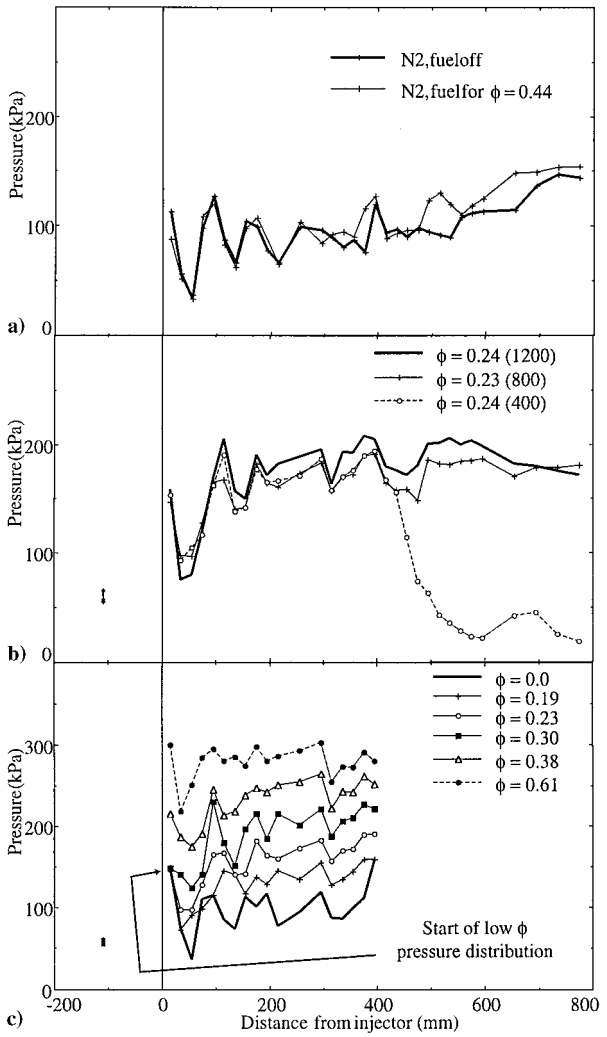

Fig. 6 T4 constant-area duct: a) N_2 shots, b) length comparison, and c) 800-mm pressure distributions (first 400 mm).

rising pressure along the combustor, modulated by the downstream influence of the injector shock system, is observed. The pressure rise is due partly to the effect of combustion and partly to the growth of the boundary layer along the combustor compressing the flow. This latter effect contributes additively to the fuel-on pressure rise.[17] Note that the increase in pressure due to the injection of the fuel is only very small in comparison to the pressure increase from the boundary-layer growth and the combustion. This can be shown theoretically using the constant volume arguments described earlier and also from experimental measurements of fuel injected into a nitrogen test gas as shown in Fig. 6a.

As the fuel equivalence ratio is increased, the pressure distribution changes to a fast initial pressure rise from the postinjector pressure level, followed by a slow growth along the combustor ($\phi = 0.29, 0.33$). For $\phi \geq 0.43$, the initial pressure rise moves upstream of the injector exit, and the pressure distribution along the entire combustor is no longer increasing, but is either steady or decaying. The latter is indicative of subsonic combustion. At the highest fuel equivalence ratio investigated, the pressure rise has moved upstream of the leading edge of the injector, exhibiting the features of a normal shock sitting in the exit of the VAG nozzle.

It is postulated from these observations that the following is occurring. For $\phi = 0.29$, separation of the combustor wall boundary layer has occurred due to the increase in pressure resulting from combustion and from the presence of the boundary layer itself. The empirical criterion for shock-induced turbulent boundary-layer separation of Korkegi[18] states that

$$P_i / P > 1 + 0.3M^2 \tag{7}$$

that is, the boundary layer separates when the local pressure P (at local Mach number M) is elevated to the incipient separation pressure P_i via shock impingement. This pressure relationship is convenient for application to the present case. Note that it agrees well with the widely used[15] Mach number relationship of Love[19] for the same phenomena, that is,

$$M_i / M < 0.762 \tag{8}$$

This can be seen by computing the pressure and Mach number downstream of a reflected oblique shock. The value of M_i / M when $P_i = P(1 + 0.3M^2)$ holds is a slowly varying function of M, equal to 0.745 for $M = 1.5$ and equal to 0.689 for $M = 3.5$ ($\gamma = 1.4$ is assumed). Equation (8) is satisfied if Eq. (7) is satisfied. The agreement between the two equations is even better for isentropic compression, where again M_i / M is a slowly varying function of M, equal to 0.747 for $M = 1.5$ and equal to 0.706 for $M = 3.5$.

It is assumed for the present combustor that Eq. (7) [and Eq. (8)] applies for isentropic compressions and for isentropic/shock compression combinations. Applying Eq. (7) for the present combustor inlet conditions, boundary-layer separation would be expected for pressures exceeding 164 kPa (that is, for pressure encountered with the $\phi \geq 0.29$ cases). Associated with the boundary-layer separation, an oblique shock train forms,[15] which elevates the static pressure to that required by the combination of combustion and the flow blockage caused by the separation. The boundary-layer separation and shock train initially originate from some position downstream of the injector, but migrate upstream until they reach the rear of the injector, where the area of the duct decreases and acts as an isolator. The increase in pressure along the duct for $\phi = 0.29$ and 0.33 suggests that supersonic combustion is occurring. For $\phi = 0.43$ and 0.55, the rapid pressure rise to levels exceeding the exit pressure is attributed to a normal shock train.[15] Subsonic combustion occurs, shown by the subsequent decay in pressure along the combustor. In addition, it can be seen that the restriction caused by the injector is no longer limiting the subsonic flow to downstream of the injector. Finally, at an equivalence ratio between 0.51 and 0.61, the injector no longer isolates the intake from the subsonic flow in the combustor so that the influence of the boundary layer separation extends upstream of the injector.

For the experiments in the shock tunnel, the influence of different duct lengths was very small. This is evidenced in Fig. 6b, which compares pressure distributions over the first 800 mm of the 400-, 800-, and 1200-mm ducts for an equivalence ratio $\phi \approx 0.23$. As already described, the 400-mm duct was created by removing the surface opposite the transducers for $x > 400$ mm, creating the strong expansion shown in Fig. 6b for that case. Where the measurements can be compared, it is seen that there is essentially no difference between the 400- and 800-mm ducts, and that the 1200-mm duct has produced a slightly higher pressure. The difference is attributed to shot-to-shot variation. The same result is observed for $\phi \approx 0.6$. The overall conclusion is that duct length in T4 has very little, if any, effect on the pressure distribution upstream of the duct exit.

Figure 6c presents the T4 800-mm constant area-duct results. Only the first 400 mm of the distributions are shown. Given the very small difference observed between the 400- and 800-mm ducts, these results will be used subsequently for comparison with the VAG results. The general trend is for a gradual increase in the entire pressure distribution with increasing fuel input. The results appear to be qualitatively very similar to the VAG case. At low ϕ, the pressure distribution rises along the duct due to boundary-layer growth and combustion. The strong pressure rise at $x \approx 100$ mm is evidence that the boundary layer has separated for $\phi \geq 0.30$. At higher ϕ (≥ 0.38), the pressure rise appears to commence upstream of the injector exit. At an equivalence ratio of 0.61, it is observed that the pressure in the combustor has only small disturbances superimposed on a slightly decaying mean (indicating that it is subsonic), except for a large disturbance near the injector (indicating that the flow could still be supersonic there). Hence, it is concluded that the flow is close to its sonic limit. This would be expected because, as discussed earlier, thermal choking in the T4 flow should occur at this equivalence ratio.

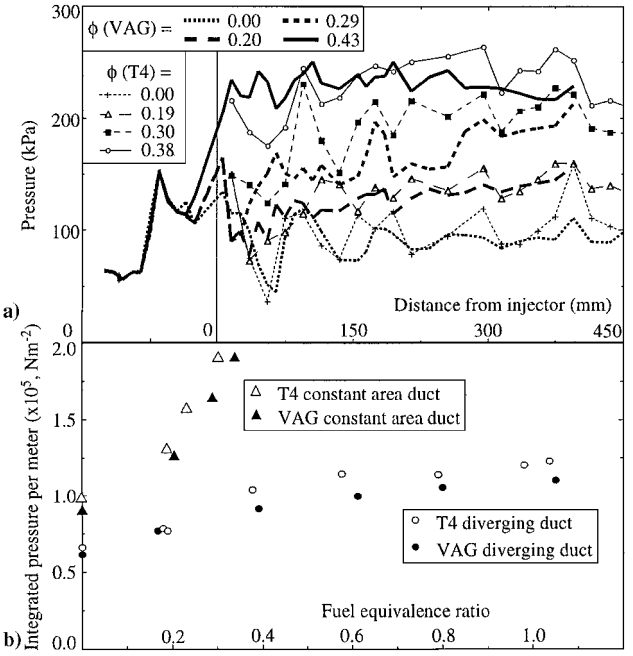

Fig. 7 Comparisons: a) T4 and VAG constant-area duct and b) constant-area and diverging-duct integrated pressure.

A direct comparison between the T4 constant-area duct results shown in Fig. 6c and the VAG constant area duct results is shown in Fig. 7a, for $\phi \approx 0$, 0.2, 0.3, and 0.4. Apart from some differences in shock structure, the two facilities agree well for the $\phi = 0$ and 0.2 cases (the mean T4 pressures are 100 ± 28 kPa and 131 ± 24 kPa, whereas the VAG pressures are 93 ± 20 kPa and 124 ± 20 kPa). Differences in the shock structure are attributed to the different flow conditions mentioned earlier, differences in the shock reflection process at the walls (due to different boundary layer thicknesses), and also slightly different duct heights between the two facilities. For $\phi \approx 0.3$, the T4 pressure distribution is higher than that of the VAG, whereas the $\phi \approx 0.4$ case shows good agreement (231 ± 26 kPa for T4 and 229 ± 11 kPa for the VAG) between the two facilities (although extrapolation of the $\phi = 0.38$ result to $\phi = 0.43$ for T4 would show higher pressures). Given the subsonic nature of the flow for the higher ϕ, caution should be exercised in drawing conclusions from those comparisons. For $\phi \leq 0.3$, however, the agreement between the facilities is encouraging.

Because of the greater fluctuations along the T4 pressure distributions, it is difficult to draw precise conclusions about the comparison between the complex flow phenomena occurring in both facilities. However, the following broad observations can be made: 1) At $\phi \approx 0.2$ and lower, supersonic combustion without boundary-layer separation appears to occur in both facilities. 2) Runs in T4 with $\phi \leq 0.30$ commence their pressure distribution downstream of the injector at the same level as the fuel-off case, whereas for $\phi \geq 0.38$ the pressure distribution starts at much higher pressures than the fuel-off case, and the origin of this rise appears to be upstream of the injector exit (this observation compares well with the VAG results, where this transition occurred for $0.33 < \phi \leq 0.43$). These observations lead to an important result: They indicate that combustion-induced boundary-layer separation (and the propagation of high pressure upstream of the injector exit) is produced and is behaving in approximately the same way in both the impulse and blowdown facilities. In other words, the short duration of the impulse facility does not limit it from simulating such phenomena.

To make a comparison between the overall results of the two facilities without the overlaid shock structure, the pressure distributions have been integrated over the duct length (the first 400 mm in the case of T4) for the equivalence ratios at which supersonic combustion is believed to be occurring (as described earlier). The results (per unit length) are presented in Fig. 7b. For the constant-area duct results (the diverging-duct results will be described later), the T4 distribution has approximately the same shape as, but lies slightly above (up to 15% at the higher ϕ), the VAG values, further indicating that both facilities are behaving similarly.

Diverging-Duct Results

To extend the comparisons to supersonic flows at higher fuel equivalence ratios, the diverging-duct combustor experiments were performed. The pressure distributions measured in the VAG diverging combustor for various ϕ are presented in Fig. 8a. The trend shown is for the pressure to decrease along the duct as the flow expands. Toward the exit of the combustor, the pressure rises sharply as the flow encounters a recovery shock to the atmospheric pressure outside the scramjet. In the same manner that was observed for the constant-area duct, the presence of fuel has altered the shock structure in the duct from the fuel-off case. For the fuel-on cases, the entire pressure distribution appears to be simply translated upward (a constant pressure value added to the whole distribution). This suggests that combustion takes place very rapidly at the start of the combustor (over the first 100 mm), and then the pressure decays due to the flow expansion. The largest increase in the pressure rise due to combustion is associated with the low values of ϕ (0.17 and 0.39). At higher ϕ, similar increases in fuel mass flux are accompanied by smaller increases in pressure.

Figure 8b presents the divergent-duct pressure distributions measured in the shock tunnel, for nominally identical ϕ to the VAG

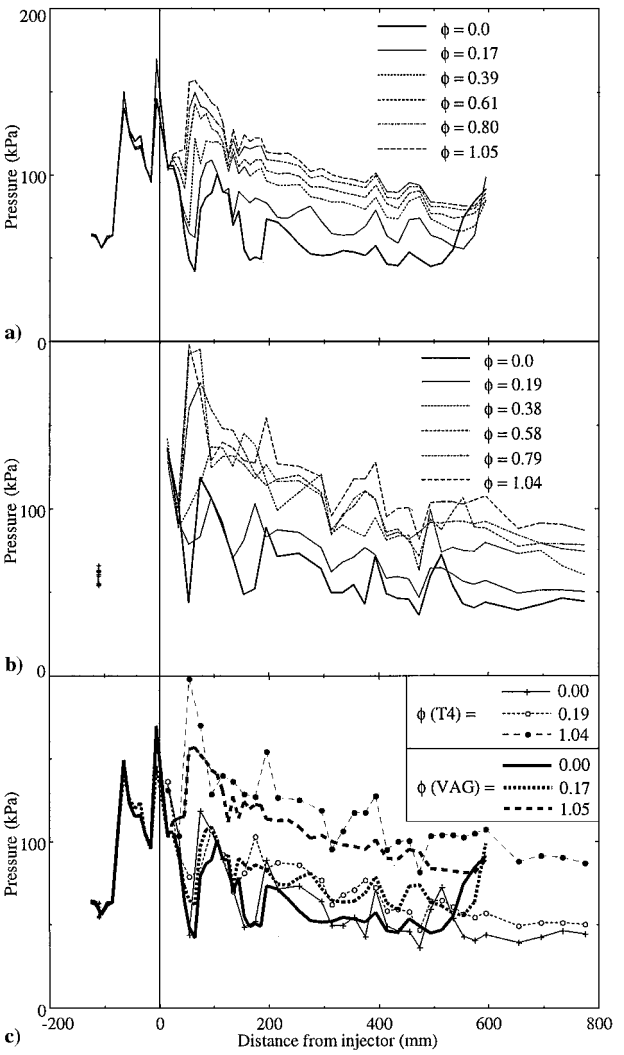

Fig. 8 Diverging duct: a) VAG pressure distributions, b) T4 pressure distributions, and c) T4 and VAG comparisons.

experiments. The features of the T4 distribution are essentially the same as the VAG case, with the exception that the T4 distributions are somewhat noisier, an effect of the much shorter flow duration. Also, no recovery shock is present in the T4 data due to the low pressure outside the combustor. A direct comparison between the two facilities is presented in Fig. 8c, for $\phi = 0.0$ and for two fuel-on cases. Agreement (to within 4% for mean pressures, see Fig. 7b) is observed between the two facilities for $\phi = 0.0$ and $\phi \approx 0.18$. For $\phi \approx 1$, however, T4 has produced higher pressure levels than the VAG.

As for the constant-area duct result, to make a comparison between the overall results of the two facilities without the overlaid shock structure, the pressure distributions have been integrated along the first 500 mm of the duct for each ϕ. The results (per unit length) are shown in Fig. 7b. The 500-mm limit was chosen to avoid the VAG pressure rise at the duct exit caused by the back pressure. Figure 7b shows the clear trend that, for $\phi \leq 0.18$, the integrated pressure agrees well between the two facilities, whereas for $\phi \geq 0.39$, the integrated pressure in the shock tunnel is consistently up to 15% higher than in the VAG, similar to the constant-area duct results. Furthermore, the effect has only a weak dependence on ϕ, unlike the constant-area duct values, which means that large uncertainties in the fuel equivalence ratio could be tolerated while still maintaining the conclusion that the pressure rise in the shock tunnel is greater than in the VAG. With regard to the issue of vitiated vs nonvitiated air, the behavior of integrated pressure with ϕ observed here agrees qualitatively with the results of Mitani et al.,[1] and Guy et al.[3]

Discussion of Results

To understand the reason for the greater measured pressures in the shock tunnel than in the VAG, we first consider the possible effect that the difference in flow conditions between the two facilities would have. In particular, for the case of equilibrium combustion, the higher initial static temperature of the VAG reactants would produce a higher temperature for the combustion products, resulting in greater concentrations of dissociated products and, hence, less net heat release and pressure rise, as compared with T4. In addition, the presence of H_2O in the VAG air would favor the reactants side of an equilibrium combustion, leading to less H_2O and more dissociated products, and lowering the VAG pressure rise relative to T4.

For example, application of the theoretical analysis described earlier to the upstream edge of the combustor indicates that, at an equivalence ratio of 0.3, the effect of the higher temperature and velocity (neglecting H_2O) of the VAG is to reduce the equilibrium combustion pressure to 82% of that in T4. Inclusion of 30% H_2O (by volume) in the freestream air in the calculation for the T4 flow conditions lowers the T4 equilibrium combustion pressure by only 8%. The difference in flow conditions is, thus, likely to have a greater effect on the far-field pressure after combustion than the direct effect of the water content.

To examine the differences between the two facilities more closely, the one-dimensional equilibrium combustion analysis described earlier is used to compute pressure distributions along the diverging combustor for both facilities, for $\phi \approx 0.4$ and 0.6.

To check the importance of skin friction and surface heat flux, pressure distributions have been calculated for the T4, $\phi = 0.38$ flow for the following four cases, all of which account for boundary-layer displacement: 1) skin friction accounted for and surface heat flux excluded, 2) surface heat flux accounted for and skin friction excluded, 3) both accounted for, and 4) neither accounted for. The results are presented in Fig. 9. It can be seen that skin friction and surface heat flux both have significant but opposing effects, with skin friction gradually increasing the pressure and surface heat flux gradually lowering the pressure. The net effect in this case is dominated by the skin friction, with a pressure distribution that has risen above the boundary-layer displacement effect only result by only 4% after 600 mm. Similar trends are found for other fuel equivalence ratios and for the VAG. Also shown on Fig. 9 are the relevant experimental data, and it can be seen that the greater the distance down the duct, the closer the theoretical analysis comes to the experimental data,

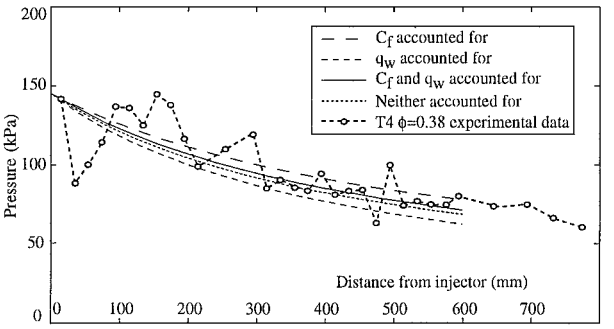

Fig. 9 T4 diverging-duct ϕ = 0.38 theoretical and experimental pressure comparisons.

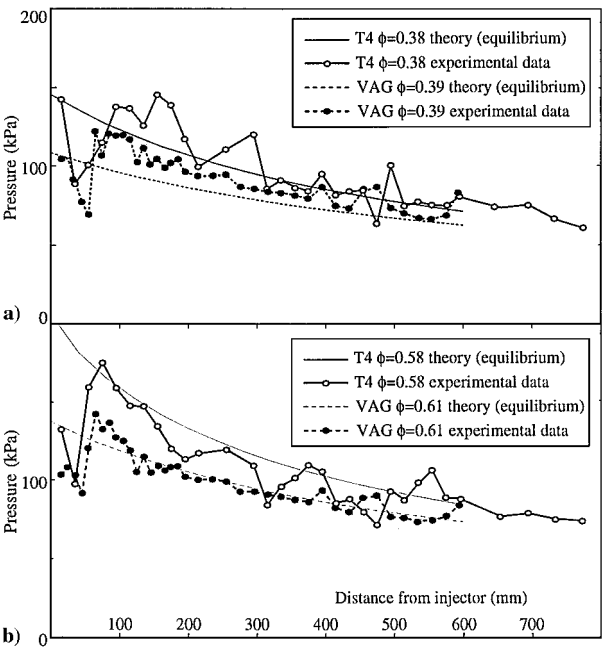

Fig. 10 T4 and VAG diverging duct theory vs experiment: a) $\phi \approx 0.4$ and b) $\phi \approx 0.6$.

supporting the earlier statement that the analysis is most useful in the far field. Closer to the injector, the agreement is not as good, due most obviously because of the presence of the shock system.

Figures 10a and 10b compare the full equilibrium-chemistry analysis, including boundary-layer displacement, skin friction, and surface heat flux, with the diverging-duct experimental data for both facilities for $\phi \approx 0.4$ and 0.6. Inspection of Figs. 10 leads to a number of conclusions. First, the theoretical pressure distributions for the VAG lie under the T4 distributions, as is the case for the experimental data. Second, the large difference just downstream of the injector between the theoretical results for each facility is reduced with increasing distance from the injector, until the smaller differences observed between the facilities in the experimental data are achieved. This reflects that, near the injector, mixing is furthest from completion and chemistry is furthest from equilibrium. Third, at the lower equivalence ratio, the theoretical pressure distributions lie in general below the respective experimental distributions (except in the vicinity of the strong postinjector expansion/shock combination), asymptoting to the experimental values as the distance along the duct increases. On the other hand, at the higher equivalence ratio, the theoretical and experimental distributions are in better agreement (particularly for the VAG) over most of the duct. Fourth, and perhaps most important, that the far-field analysis agrees extremely well with the far-field experimental data at both equivalence ratios and in both facilities means that, after taking into account the differences in freestream conditions, the far-field pressure rise due to combustion is the same for each facility (to within experimental uncertainty).

Conclusions

A series of experiments have been performed in which supersonic combustion has been compared between a vitiation-heated blowdown tunnel and a free-piston shock tunnel. Comparisons for combustion in a constant-area duct showed reasonable agreement between the two facilities for fuel equivalence ratios less than approximately 0.3, with measured pressures up to 15% higher in the shock tunnel than in the vitiation-heated tunnel. The measurements provide the important result that boundary-layer separation and its associated effects occurs and behaves similarly for the two types of facility. For higher ϕ, the results indicate that boundary-layer separation combined with combustion heat release caused the duct to choke, leading to subsonic flow. Experiments in a diverging combustor extended the equivalence ratio range to 1.05. The two facilities again showed reasonable agreement at low ϕ, whereas at high values the shock tunnel produced pressure distributions up to 15% higher than the vitiation-heated tunnel, in agreement with the constant area duct and with other work.[1,3] A quasi-one-dimensional equilibrium chemistry combustion analysis that accounts for boundary-layer effects gave excellent agreement with the experimental data in the far field, with the main conclusion being that the observed differences between the facilities can be explained by the difference in combustor inlet conditions (including water content) between the facilities. However, the effect due to vitiation was dominated by the influence of the difference in other flow parameters, and could not be distinguished.

Acknowledgments

The authors gratefully acknowledge the financial support of the Australian Space Office and the assistance of K. Dudson, J. Gisa, K. Kudo, A. Murakami, and S. Sato in the experiments.

References

[1]Mitani, T., Hiraiwa, T., Sato, S., Tomioka, S., Kanda, T., and Tani, K., "Comparison of Scramjet Engine Performance in Mach 6 Vitiated and Storage-Heated Air," *Journal of Propulsion and Power*, Vol. 13, No. 5, 1997, pp. 635–642.

[2]Mitani, T., "Ignition Problems in Scramjet Testing," *Combustion and Flame*, Vol. 101, No. 3, 1995, pp. 347–359.

[3]Guy, R. W., Rogers, R. C., Puster, R. L., Rock, K. E., and Diskin, G. S., "The NASA Langley Scramjet Test Complex," AIAA Paper 96-3243, July 1996.

[4]Masuya, G., Komuro, T., Murakami, A., Shinozaki, N., Nakamura, A., Murayama, M., and Ohwaki, K., "Ignition and Combustion Performance of Scramjet Combustors with Fuel Injection Struts," *Journal of Propulsion and Power*, Vol. 11, No. 2, 1995, pp. 301–307.

[5]Stalker, R. J., "Shock Tunnels for Real Gas Hypersonics," AGARD Conf., Aerodynamics of Hypersonic Lifting Vehicles, Symposium of the AGARD Fluid Dynamics Panel, AGARD CP428, Bristol, UK, 6–9 April 1987.

[6]Boyce, R. R., Paull, A., and Stalker, R. J., "Unstarted Inlet for Direct Connect Combustor Experiments in a Shock Tunnel," *Journal of Propulsion and Power* Vol. 16, No. 4, 2000, pp. 726–727.

[7]Miyajima, H., Nakahashi, K., Hirakoso, H., and Sogame, E., "Low-Thrust LO2/LH2 Engine Performance with a 300:1 Nozzle," *Journal of Spacecraft and Rockets*, Vol. 22, No. 2, 1985, pp. 188–194.

[8]McIntosh, M. K., "Computer Program for the Numerical Calculation of Frozen and Equilibrium Conditions in Shock-Tunnels," Dept. of Physics, ANU Internal Rept., Australian National Univ., Canberra, ACT, Australia, Sept. 1968.

[9]Lordi, J. A., Mates, R. E., and Moselle, J. R., "Computer Program for the Numerical Solution of Nonequilibrium Expansions of Reacting Gas Mixtures," NASA CR-472, 1966.

[10]Morgan, R. G., and Stalker, R. J., "Fast Acting Hydrogen Valve," *Journal of Physics E: Scientific Instruments*, Vol. 16, No. 3, 1983, pp. 205–207.

[11]Wendt, M., "Supersonic Combustion in a Constant Area Duct," Ph.D. Dissertation, Univ. of Queensland, Brisbane, QLD, Australia, 1994.

[12]Shapiro, A. H., *The Dynamics and Thermodynamics of Compressible Fluid Flow*, Vol. 2, Ronald, New York, 1954, p. 1093.

[13]Edenfield, E. E., "Design of a High Reynolds Number Mach Number 8 Contoured Nozzle for the Hypervelocity Wind Tunnel (F)," Arnold Engineering Development Center AEDC-TR-72-48, Arnold Air Force Station, TN, Aug. 1972.

[14]Hirschfelder, J. O., Curtiss, C. F., and Bird, R. B., *Molecular Theory of Gases and Liquids*, Wiley, New York, 1954, p. 604.

[15]Heiser, W. H., and Pratt, D. T., *Hypersonic Airbreathing Propulsion*, edited by J. S. Przemieniecki, AIAA Education Series, AIAA, Washington, DC, 1994, pp. 482, 240, 252.

[16]Stull, D. R., and Prophet, H., "JANAF Thermochemical Tables," US National Bureau of Standards, Washington, NSRDS-NBS 37, June 1971.

[17]Wendt, M., Jacobs, P. A., and Stalker, R. J., "Displacement Effects and Scaling of Ducted, Supersonic Flames," *Combustion and Flame*, Vol. 116, No. 4, 1999, pp. 593–604.

[18]Korkegi, R. H., "Comparison of Shock-Induced Two- and Three-Dimensional Incipient Turbulent Separation," *AIAA Journal*, Vol. 13, No. 4, 1975, pp. 534, 535.

[19]Love, E. S., "Pressure-Rise Associated with Shock-Induced Boundary-Layer Separation," NACA TN 3601, Dec. 1975.